

Publication Year	2018
Acceptance in OA@INAF	2021-01-21T11:46:31Z
Title	Chasing passive galaxies in the early Universe: a critical analysis in CANDELS GOODS-South
Authors	MERLIN, Emiliano; FONTANA, Adriano; CASTELLANO, MARCO; SANTINI, Paola; Torelli, M.; et al.
DOI	10.1093/mnras/stx2385
Handle	http://hdl.handle.net/20.500.12386/29917
Journal	MONTHLY NOTICES OF THE ROYAL ASTRONOMICAL SOCIETY
Number	473



4.1 The SED-Þtting method

The SED- tting has been performed on the 19 bands catalogue de
evolving, with a negligible amount of star-formation activity. scribed in Section 2 using our codehot in which we have implemented the TH models in addition to standardhodels. The same SED- tting technique has been used in several previous studies

We performed our search for passive galaxies in the GOODS-South (Fontana et al2004 2006 Grazian et al2006 Maiolino et al.2008 Santini et al 2012 Dahlen et al 2013 Castellano et al 2014 2016 and it is similar to that adopted by other groups in the literature (e.g. Dickinson et al 2003 Ilbert et al. 2013; however, the adoption of the abruptly guenched SFH is novel.

As described above, the TH library consists of a grid of models with constant SFR for a time tourst after which the SFR is set to zero. The models have been created using Bruzual & Charlot (2003 BC03) libraries and adopting a Salpet 4959 IMF. Ages are computed from the onset of SFR, which means that any model probability p(2) of any tted model. The probabilityp(2) is is star-forming from age 0 to age t_{bursb} and passive for age thurst. Only ages less than the age of the Universe at a given redshift are allowed. The burst duration burst spans several values (0.1, 0.3, 0.6, 1.0, 2.0 and 3.0 Gyr) as well as metallicitæs (= 0.2, 0.4, 1). For each value oft_{burst} dust is included adopting C00 or Small Magellanic Cloud (Prevot et al984) attenuation curves, limited within the following physically motivated values:

(i) 0 < age
$$t_{burst}$$
: 0 < E(B Š V) 1
(ii) age> t_{burst} : 0 < E(B Š V) 0.2

(this choice mimics the expected drop of dust content in a quenched factor, in order to have the 2 of the best-tting solution equal to galaxy after the end of the star-forming activity). The full library consists of 3.13 millions models, and the quasi-logarithmic step in age results in a larger number of star-forming model (8) per cent indeed have age t_{burst}).

Another important ingredient in computing the SED of highsigni cantly to the observe &band and IRAC uxes (e.g. Navyeri et al.2014 Paci ci et al.2015. As rst presented in Castellano et al. (2014), the contribution from nebular emission has been inserted in are computed in the same way. zphotfollowing Schaerer & de Barro 2009. Brie y, nebular emission is directly linked to the amount of hydrogen-ionizing photons in the stellar SED (Schaerer & Vacda98) assuming an escape fraction $f_{asc} = 0.0$. The ionizing radiation is converted in nebular continuum emission considering free-free, free-bound, and H two-photon continuum emission, assuming an electron temperature than the duration of the burstt_{burst} and must have a probability $T_e = 10000 \,\mathrm{K}$, an electron densite = $100 \,\mathrm{cm}^{3}$, and a 10 per cent helium numerical abundance relative to hydrogen. Hydrogen lines p from the Lyman to the Brackett series are included considering case B recombination, while the relative line intensities of He and met-bility of the candidates by requiring that no plausible star-forming als as a function of metallicity are taken from Anders, Fritze-von Alvensleben & de Grijs 2003).

However, the computation from rst principles of this contribusamples. For this reason we choose to adopt two different paths:on the absolute value of the probability 2), not on the density described above. We will analyse our sample separately with both along the (many) free parameters. libraries.

be equal to zero in passive candidates, and (equivalently) the galaxylibrary, consisting of 2500 star-forming models haviring magnifor ages shorter than t_{burst}, the galaxy is star-forming – these models can be described reasonably well both as starburst galaxies of the distribution observed in each CANDELS pass-band; the full with a relatively small amount of dust (i.e. the usual Lyman Break catalogue therefore consisted o£5 000 mock objects. Then, we

larger than t_{burst} these models describe galaxies that are passively

4.2 The selection criteria

eld starting from theH-detected catalogue, and using the photometric data described in Section 2. First of all, we selected all the sources in G13 havined 160 < 27, with simultaneous 1 detection in Ks (Hawk-I), IRAC 3.6 and IRAC 4.5µm bands. We also excluded from the selection any source with defects or unclear classi cation (relying on the CANDELS agging). Finally, we added the K/IRAC-detected sources to the list. On this sample, we have performed the SED- tting process described above.

The selection is done using the information contained in the

simply computed as the probability that the observed(computed on all bands) is due to normally distributed errors (the number of free parameters used in the calculation is actually 1, with N the available number of bands for each object, as 1 degree of freedom is used to normalize the spectrum). Similarly to what has been done in several previous works (e.g. Papovich, Dickinson & Ferguson 2001; Fontana et al. 2009; Santini et al. 2015), the procedure to estimate the is iterative. The of each object is rst evaluated on its photometry, and then the uncertainties on the observed bands are all increased by a constant the choice of the best- tting solution) is used to take into account the limitations of the template models, that may lead to relatively large ² (the average ² is indeed 3) despite an overall good t.

We note that this approach is particularly conservative, as it widens signi cantly the allowed parameter space, and hence the possibility that a given object is classi ed as both passive and star-forming. Uncertainties on all the other relevant physical quantities in the tare computed in the same way.

Our proposed method uses the probability by requiring that the following two conditions are ful lled:

(i) no star-forming solutions with a probability higher than a xed thresholdpsF exist;

(ii) the best-tting solution is characterized by an adtarger than the duration of the burstt_{burst} and must have a probability p 30 per cent.

The rst of these two criteria enforces the reliability and credibility of the candidates by requiring that no plausible star-forming solution alternative to the best-t one exists; in practice, this is obtained by looking at the probability (2) of every model inside our multiparameter grid (that includes dusty star-forming). 1. This boost of the photometric uncertainties (that does not change galaxies is the proper inclusion of emission lines, that can contribute signi cantly the allowed parameter space, and hence the possibility

our multiparameter grid (that includes dusty-star forming models as tion is not easy, and it has not been tested on large spectroscopiowell as passive ones). We explicitly note that our criterion is based we build models both without emission lines, as done in most of of the resulting models in the parameter space, as the latter would the published analysis so far, as well as including emission lines, asbe indeed heavily altered by the (arbitrary) sampling of the models

To assess the value ps, we used a set of dedicated simulations, The crucial output parameters of the t are the SFR, which must proceeding as follows. We created a mock catalogue using the TH age, that must be compared with the duration of the SF activity: tudes of 23, 24 and 25. Each of these models was then replicated 10 times adding observational noise, consistently with the scatter Galaxies) and more reddened galaxies – while for ages de nitely used the TH library to t these models. Around 1200 of them turned

out to have a passive best-t, showing that the effect of noise and models degeneracy can turn a star-forming observed source into a passive t, with some 5 per cent of chances. Our goal was therefore to make sure that the chosen criteria are stringent enough to avoid that any of these sources is con rmed as passive after the probabilistic selection. Unsurprisingly, these objects also had a non-zero probability of being tted with a star-forming solution, although with a worst 2 than the passive best-tting one; we found that the lowest probability of a star-forming solution is 12 per cent. Considering that the simulation is an idealized case and in real photometric catalogues the uncertainties due to blending or varying depth must be taken into account, we decided to apply a more conservative threshold of $p_{SF} = 5$ per cent.

As we show in the following, the effects of this rst condition depend dramatically on the range of redshifts allowed in the error analysis. On the other hand, the second condition is signi cantly affected by the inclusion of the emission line in the spectral library. We list below the different samples resulting from the application of these alternatives.

are too faint to be observed spectroscopically.

We therefore apply our SED-tting technique to t all the objects atzcanders > 3, utilizing the TH models without emission lines and applying the selection criteria described above.

This way, we single out 30 red and dead candidates. This approach is analogous to previous works (e.g. Fontana e2009): we use models with no emission lines and perform the scan of star-forming alternative solutions only at the best-tting photometric redshifts. For these reasons, in the following we will consider this set of objects ourreference sampleThese objects span a redshift range between 3.0 and 4.7, and have IRAC magnitudes<28n_{4.5} < 26 (corresponding to stellar masses between and 2 x 10¹¹ in our t). Five of them havez_{CANDELS} > 4 (IDs 3912, 5592, 10¹⁰ M . The 30 selected objects attedetected (while none of the A full description of their physical best-tting parameters is shown in Appendix A, along with their images in the CANDELS data set (Appendix B) and full SED and resulting best-tting spectrum (Appendix C).

It is important to remark that the condition that the probability of star-forming solutions is less thanger = 5 per cent has a dramatic effect of the selection of candidates. Indeed, the number of objects that have a formal best-tting passive solution is much larger namely 482 candidates. (Aper cent of the whole G13 catalogue, and 94 per cent of alk > 3 galaxies). Most of these candidates are, of course, faint sources with detections at very felevels in theK and IRAC bands whose t is degenerate, i.e. that can be tted nearly equally well by star-forming or passive solutions. Indeed, almost all from the intensity of the ionizing ux in the spectrum, such that the of the objects in the nal reference sample have obset/v,el-RAC 3.6 and 4.5 magnitudes25, with S/N, respectively, larger than 20, well above the detection limit. This rst example highlights the importance of the S/N in the credibility of the identi cation, on which we shall expand below.

Figure 2. Probability (p(²), upper panels) and (BŠV) (lower panels) as a function of [ageš t_{burst}] of all the possible solutions in the SED- tting process, for three red and dead candidates in the reference sample (IDss: 4.2.1 The selected reference sample

The rst t has been performed keeping the redshift xed at the CANDELS value (i.e. spectroscopic redshifts when available, photometric redshifts otherwise, the latter obtained as a median of nine independent photo's determinations; see Dahlen et 2013). For function of their density. All the solutions have age tours as required all our objects, this corresponds to the photometric redshift, as they to be classi ed as passive in this approach. Galaxies excluded from the selection, on the other hand, have been tted by at least one model with t_{burst}, i.e. still star-forming, with a probability > 5 per cent (not shown). [A colour version of this gure is available in the online version.]

In Fig. 2 we show the outcome of this procedure for three objects belonging to the reference sample (with additional information, to be explained in the next section); the whole sample is shown in Appendix D. For each object, we plot the probabilities of all the SED-tting solutions (shaded as a function of their density), and the corresponding UV extinctions, as a function of the time passed from the end of the SF burst; the candidates have solutions with high probability and low extinction well after the quenching of the activity. The extinction tends to anti-correlate with time, because 6407, 9209, 23626); these all have best- tting masses larger than of the way our models are built, but also because a red object can be tted with a young dusty model or with an old model without K/IRAC-detected additional sources passed our selection criteria). dust, so the two possibilities are somewhat degenerate and only the goodness of the t (namely the²) can disentangle them.

4.2.2 Including the emission lines

We then repeated the analysis, but this time using the TH spectral modelsincludingemission lines.

In this case, we identify only 10 objects satisfying the selection criteria. As in the previous case, the requirement on the (low) probability of the star-forming solution is very effective in removing potential candidates at low S/N (we identify a total of 194 candidates with passive best-tting solutions).

We remind here that the lines are computed self-consistently resulting SED of a quiescent galaxy is by default identical to that obtained without emission lines. As a consequence, all the objects 10 and 6. Clearly, a robust analysis is possible only for galaxies selected as passive in this 'emission lines sample' are also part of the reference sample by construction.

> On the other hand, of the 20 candidates of the reference sample that are not included in the emission lines sample, 12 have a

models without emission lines, so that a proper comparison can be more appropriately performed considering the whole reference sample. Therefore, we keep it as our ducial selection.

4.2.3 Free redshift selection

As already pointed out, the analysis described above assumes that the redshift is xed at the CANDELS photometric estimate. However, for galaxies that have a very steep spectrum and are undetected in many of the optical images, the possibility of degeneracies among the spectral templates due to low S/N and poor sampling, and/or by the adoption of incorrect templates, may lead to substantial uncertainties in the photoz-that need to be taken into account. To this aim, we repeat again the SED-tting procedure on the reference \mathbb{S} sample, but leaving the redshift free to vary around the best-tting CANDELS value in the whole redshift range where the probability p(z) of having an acceptable t is above 1 per cent.

We note that since the best-tting photometric redshift has not been computed with the TH library, it is in principle possible that the best-tting photometric redshift obtained using the TH library

However, most galaxies also have star-forming solutions at different (typically lower) redshifts, with > 5 per cent. Only two galaxies, IDs 10578 and 22085, are left as reliable passive candidates, with no probable stor forming a left. of course, this does not mean that no other candidate is reli-

able as a 'real' passive object. Indeed, the consistency between the best-tting solutions leaving free to vary and the one obtained at $z_{\sf CANDELS}$ is reassuring; furthermore, we will show in the next best-tting solutions leaving free to vary and the one obtained cantly affect the shape of the spectrum (as sampled by the broad-section that most of the objects in the reference sample have no detectable FIR emission, ensuring that most of them can be considered. as robust red and dead candidates. Nevertheless, using the present day state-of-the-art facilities and methods, it is still not possible to rule out the possibility that some low-redshift, dust-reddened starsolution, and hence do not pass our probabilistic selection criterion forming objects are erroneously identi ed as high-redshift passive galaxies with 100 per cent certainty. The best we can do is try and reduce the risk of contamination using all the available information, come (see Section 6).

sources already discussed in F2g.which passed three different levels of our selection criteria: top to bottom, ID22085, which surinteresting particularly when compared to the results of a standard vived thez-free selection and is one of the two strongest red and dead candidates; ID18180, which passed the emission line selec Fig. 3 shows the stellar masses and redshifts of the selected tion but has a star-forming solution at a redshift different from the dots). This may be expected because the ambiguity between the (which is always passive) as a red line, along with the best star-

As a summary of the free selection and a nal summary of the

In principle, spectral templates including emission lines are expected to be a more accurate representation of the real spectra, and $4.3\,$ Fir ßuxes

the intensity of such lines is expected to increase at high redshift, To further reduce the risk of including dust-obscured star-forming so that the 10 objects that are classi ed as passive even including solutions in the reference selection, we perform a sanity check on the emission lines should be regarded as more reliable. However, the Herschelimages and catalogues described in Magnelli et al. the recipes adopted here to compute the emission lines from the (2013). The FIR images are shallower than the optical and NIR SED have not been extensively tested or veri ed, especially in high ones, but they can nevertheless provide a hint on the real nature redshift galaxies. In addition, most previous works adopted spectral of these objects; and indeed, detectionblerschelbands occur in

Figure 3. Redshift versus mass distribution of the red and dead selections. Cyan points refer to objects having 5.5 and a passive best-tting solution (both in the t including emission lines and in the one without them), but excluded from the reference sample because of the existence of different, is different from the of cial CANDELS one. Reassuringly, we no erence sample (30 candidates surviving the probabilistic selection; the void that most of the candidates still have best- t solutions with zero star squares mark the 10 sources selected also using the library including nebular formation activity, at redshifts similar to the CANDELS one. lines emission); red stars: the two candidates surviving the after the g. See the text for more details. [A colour version of this gure is available in the online version.]

star-forming best-tting solution with emission lines (i.e. best-t burst) with signi cant SFRs (typically 30-50 M/yr). The physical origin of this difference can be understood looking at the SEDs shown in Appendix C. The intense emission lines signi band Iters) beyond 4000 Å, implying a weaker break and yielding a shallower slope in the rest-frame infrared region.

The remaining eight objects still have a best-tting passive solution, but also an increased probability of having a star-forming p < 5 per cent (see the table in Appendix A).

Looking at Fig.D1, one can see how in the emission lines sample (blue dots) four sources are likely to be passive since more than e.g. checking the FIR uxes, while waiting for even deeper data to 100 Myr (IDs 2782, 18180, 22085, 23626), while the other six might have quenched their SF activity very recently. In the reference sample (red dots), most of the sources have solutions suggesting whole procedure, Fig4 shows the tted SEDs of the same three very recent quenching, while only four are more likely to be passive since more than 100 Myr (IDs 3973, 4503, 7526, 7688). This is selection using decaying SFH histories (see Section 5).

candidates. The emission lines sample sources (empty squares) are ANDELS one; and ID7526, a 'standard' object in the reference among the most massive objects in the reference selection (bluesample. In each panel, we plot the best-tting model-atz_CANDELS passive and star-forming solution is increased by the somewhat forming model at any redshift (blue line). The corresponding problower S/N of the faintest among the 30 objects in the reference ability distributions can be inferred from the inner boxes.

Figure 4. Fitted SEDs of the three candidates reported in Fign the reference sample, and compared probabilities of all the solutions (inner panel), in the freæ t. In each panel, the red line is the best passive solution at the CANDELS photometric redshift, and the blue line is the best star-forming solution (at a different redshift); the dots in the inner panel refer to the corresponding probabilities. Top: ID22085, a strong candidate surpassing Cappelluti et al. 2016, which directly links X-ray emitters to the all the selection criteria: the best star-forming solution (obtainez at 3.4) has probability < 5 per cent, so this object can safely be considered passive even letting its redshift freely vary in the t. Middle: ID18180, despite having mostly passive solutions with very high probabilities, it also has a few star-forming solutions with > 5 per cent (at 3.1), so it is formally excluded from the most stringent selection. Bottom: ID7526 (which is part of the reference sample, but fails the emission line t selection) has many high-probability star-forming solutions at various redshifts. [A colour version of this gure is available in the online version.]

many cases of passive candidates detected with other methods (see Section 5).

We rst perform a spatial cross-correlation between the and coordinates of the passive candidates and the 24MIPS catalogue. We indithat two among them, IDs 3973 and 10578, have very close counterparts (below 1 arcsec), while none of the remaining 28 have one within a radius of 3.0 arcsec (the FWHM of MIPS 5s7 arcsec, but the catalogue has been obtained using IRAOB priors with FWHM 1.6 arcsec, so this minimum distance is enough to exclude the detection of 24m ux). We note that ID10578 is indeed one of the 'strongest' candidates in our reference sample. since it has survived the whole selection process, including the freez SED- tting – meaning that no star-forming solution exists at any redshift with probability above 5 per cent. Emission is detected at the position of the two sources also at longer wavelengths (100, 160 and 250µm) on the Herschel PEP-GOODS (Lutz et a 2011) and HerMES (Smith et al2012) blind catalogues; however, possible associations become more common, given the increasing width of the PSFs: at 100µm four sources have matches below the FWHM of 6.7 arcsec, at 160m 11 sources have matches below the FWHM of 11.0 arcsec, and at 250m 16 objects have a match below the FWHM of 18.1 arcsec. A visual inspection on the Herschel maps always hints at different possible objects as the origin of the detected uxes, as many other-detected galaxies lie close to the considered

To further strengthen the analysis, we have also checked a new ASTRODEEPMIPS/Herschelcatalogue by Wang et al2(16), which is deeper than previous catalogues particularly in the SPIRE bands, and uses the G18-band detections as priors. Using this catalogue, it is therefore possible to directly link each source to its measured FIR ux. The two candidates identi ed above as having clear MIPS/Herschelcounterparts are also recognized as FIR emitters in this new catalogue, while none of the other red and dead 2000 per second detections. candidates is associated with a detectable schelsource.

Herschelsource, so that it is almost impossible to discern the actual

origin of the FIR emission.

Finally, we checked a stack of the 28 non-associated sources thumbnails from the Herschelmaps, nding no trace of detectable ux in any of the considered bands.

Summarizing, it is fair to conclude that there is no emission at 24 µm evidently linked to 28 out of 30 sources in the reference sample. Two objects instead clearly have FIR counterparts. In principle, this might be due to their wrong identi cation as passive in the SED- tting process. However, as discussed above, the uncertainty in the classi cation dramatically worsens for objects with low S/N, while both the two galaxies are very bright (ID 3973 has SAN 17.3 and S/N = 49.9, and ID 10578 has S/N = 166.8 and S/N = 528.9). A possible different explanation for their strong FIR emission might be the presence of a dust-obscured active galactic nucleus (ACN) heart in (AGN) hosted in a recently passivized galaxy. In this case, while the stellar content would yield a passive spectrum in the optical and NIR wavelengths, galactic dust absorbing and re-emitting part of the X radiation from the nuclei could cause the observedschel uxes. To test this hypothesis, we check **tob** and racatalogue by H-detected sources in G13. As it turns out, both the two sources are identi ed as X-ray emitters in the catalogue. Also, in our analysis they are tted with a relatively high amount of extinction (B Š V) = 0.2 for ID3973 and 0.3 for ID10578]. This leads to the interesting speculation that these two galaxies indeed seem to have recently become passive, but still retain an active radiating nucleus, and large amounts of dust which cause the observed FIR strong emission. For these reasons, we decide to keep the two sources in the reference

tive galaxies (see e.g. Giallongo et 2015), while our SED libraries are solely based on stellar tracks.

4.4 Properties of the red and dead candidates

Four galaxies in the reference sample have been observed spectroscopically: IDs 4503 (Mobasher, priv. comm.), 9209 (Cassata et al. 2015), 10578 (Vanzella et al2008), 19505 (VANDELS, but the observations and analysis are not completed yet). In all the CRITERIA cases z_{spec} is close toz_{CANDELS}, except for 10578 z_{spec} = 3.89, z_{CANDELS} = 3.06). However, all of these spectra have poor-quality ags, so that they cannot be taken as strong constraints to our aims; and the observedJL andiHM diagrams), and with those obtained the only exception might be ID19505, which shows a broad line at 5640 Å that can be interpreted as a strong Lymæmission. This would imply $z_{\text{spec}} = 3.6386$; tting the observed photometric data at this redshift yields an SED which is very similar to the one 5.1 The UVJ selection at z_{CANDELS} = 3.33, but with a worse ², which would exclude the object from the selection.

Considering the area of the GOODS-South deep eld (173 arcmin), the 30 passive candidates would imply a number density of 0.173 passive objects per archinatz > 3 and above the detection criteria. The corresponding total comoving number density in the redshift interval 3 z < 5 is of 2.0×10^{55} Mpc^{S3}. Fig. 5 shows a comparison between the number density of passive a selection based on the speci c SFRs. high redshift objects inferred from these study and the one found by S14: applying their same mass selection criterio Mof 10^{10.6} M ,³ and considering their redshift bin 0.65log(1 + z) < 0.72, we nd a number density of 1.0×10^{55} if we consider the whole reference sample, and of6.0x 1056 if we only include the emission lines selection. These densities are slightly lower than the 1.78 x 10^{\$5} value found by \$14 – which is unsurprising given with the value found by Muzzin et al2013.

Figure 5. Number density of red and dead candidates with log[M/M] > 10.6 in the redshift bin 0.6 log(1 + z) < 0.72, from this work (blue star: reference sample; magenta star: 'emission lines' selec-Figure 6. UVJ diagram forz_{CANDELS} > 3 sources, computed adopting the tion), compared to the results by S14 (red squares). Our mass estimates ar standard -models to derive the rest-frame magnitudes. The passive selection corrected to match the analysis by S14, who assumed a Chabrier IMF rather region is de ned by (U Š V) > 0.88x (V Š J) + 0.59, (U Š V) > 1.2 and than a Salpeter IMF. See the text for more details. [A colour version of this gure is available in the online version.]

The passive selection to derive the rest-frame magnitudes. The passive selection is dened by (U Š V) > 0.88x (V Š J) + 0.59, (U Š V) > 1.2 and (V Š J) < 1.4 (Whitaker et al.). Yellow points are the whole sample of z > 3, Ks+3.6+4.5 \mm H-detected galaxies from G13. Cyan small dots refer to the objects having a passive best- ting model, both with and without the inclusion of the emission lines in the TH library. Blue large dots are the wavelength range can be also typical of AGNs hosted in young, ac-30 galaxies in the reference sample, with empty squares indicating the 10.8 logical properties. 30 galaxies in the reference sample, with empty squares indicating the 10 good sources selected also including nebular emission lines. The red stars referous to the candidates surviving the free selection. Finally, empty circles referous to the candidates surviving the free selection. Finally, empty circles referous to the candidates surviving the free selection. Finally, empty circles referous to the candidates surviving the free selection. Finally, empty circles referom to the candidates surviving the free selection. Finally, empty circles referom to the candidates surviving the free selection. Finally, empty circles referom to the candidates surviving the free selection 5). Not all the galaxies in the selection sample because some models have very similar rest-frame properties and colours, so that the symbols overlap. [A colour version of this gure is available in the online version.]

5 COMPARISON WITH OTHER SELECTION CRITERIA

In this section we compare our results with those that can be obtained using other selection criteria (namely the rest-frame) diagram from the observed JL and iHM diagrams), and with those obtained in similar recent studies. wavelength range can be also typical of AGNs hosted in young, ac- 30 galaxies in the reference sample, with empty squares indicating the 10 2

It is interesting to check which sources would be identied as passive using a more standard approach. To this aim, we started anew from the G13 catalogue, and perform the SED-tting on the photometric data set, again keeping the of cial CANDELS redshifts, but now using a typical library of -models, without the inclusion of nebular lines. On this sample we tested both the standard criterion and

Fig. 6 is a UVJ diagram in which, for the sake of clarity, we only plot the z_{CANDELS} > 3 sources. In this plot we use the rest-frame colours obtained from the model tting. We display the position in the UVJ plane of the objects in our reference sample (blue dots; the 10 objects also selected with the library including nebular emission are highlighted with empty squares). Here we use the rest-frame colours of the best-tting models; we checked that using colours their more relaxed selection criteria – and are broadly consistent computed interpolating the observed uxes (shifted at the redshift of the source), e.g. using zy, yields qualitatively similar results, although with a larger scatter in the distribution. Reassuringly, it is clear that most of the objects that are selected as passive with the UVJ approach are also selected with our technique. However, some account the fact that we adopt a Salpeter IMF rather than a Chabrier IMF as contamination is present, as a few objects fall inside this region but are not selected in our reference sample: these objects are discarded

³ We apply a scaling factor of 0.24 dex (e.g. Santini et al.) to take into in S14.

in our case due to the existence of possible star-forming solutions with p > 5 per cent. In addition, a non-negligible number of our candidates in the reference sample fall outside (below) of the passive region, in the region where recently quenched sources are expected to lie (as discussed in Section 3). This con rms that the adoption of simple -models and colour criteria may fall short in singling out a complete sample of red and dead objects, and we therefore conclude that the choice of a more sounded SFH analytic shape like the top-hat we adopted in this study can have signi cant impact on the selection of realistic candidates of passively evolving objects at high redshift.

In the same Fig6, we also code the objects according to their estimated sSFR in the t. We selected as red and dead candidates the objects having speci c rates sSRR10^{Š11} yr^{Š1}: with this criterion, and again requiring_{CANDELS} > 3 and Ks+3.6+4.5 1 detection, we single out only 10 objects, marked as open circles in the gure. We notice that only 5 out of 10 are present in the TH selection: they are IDs 2782, 7526, 8785, 17749 and 18180. Their best-tting values are similar to those obtained with the TH libraries. Snapshots showing the other ve sources included in the selection and not in the reference TH selection are shown in Hid; we note that ID 34275 is only clearly visible in the I-band image and might be a spurious detection from a close-by star, while IDs 2032, 5501, 22515 and 34636 have not been included in the TH selection despite having best to as passive objects, because star-forming solutions with p > 5 per cent are present.

Interestingly, none of the vez > 4 red and dead candidates in the reference selection is identi ed as passive with threeodels criteria. Two of them, IDs 3912 and 23626, are tted as sources 1.3 Gyr and 500 Myr, respectively, missing the selection because of estimated sSFR slightly higher than the chosen thresh shifts are small (0.3 mag) and typically more pronounced in the J old $(6.3 \times 10^{\$11} \text{ and } 4.2 \times 10^{\$11} \text{ yr}^{\$1})$. The other three objects (IDs 5592, 6407, 9209) are tted as young (age800 Myr) starforming sources with sSFR10^{Š10} yr^{Š1}. The ² of the ts with the -models and the TH models are similar. Again, if our modelling is correct, all these are good examples of the kind of objects dis- 5.2 Diagnostic planes with observed colours cussed in Section 3: young galaxies in the early Universe which have quenched their short SF activity abruptly, just before the Fig. 8 shows the result of the selections on diagnowable and iHM time they are observed, and are identi ed as still (slightly) starforming in a standard t because of the limitation of the chosen tting model.

Fig. 7 (top panel) displays the shifts in the /J diagram positions for the objects belonging to the reference sample, when tted with different libraries of models. The shifts are typically small, of the order of 0.1-0.3 mag (generally consistent with the uncertainties in the relevant observed colours). Noticeably, they tend to affect the V Š J colour more than the J Š V colour. This is basically due to the fact that the t is much more robustly constrained in the region of the observed visible and NIR (covered by the ACS and of the diagram, many others are found having slightly bluer ob-WFC3 bands), which straddle the rest-frable V break at 3, than in the reddest part of the spectrum, since the two 5.6448.0 IRAC bands have the poorest S/N. This allows larger variations in the V S J colour, as shown by the two examples reported in the bottom panels of the same gure. We also note a systematic 5.3 Comparison with previous samples effect between the two libraries, as most of the candidates with a red [U Š V]_{rest} have bluer [/ Š J]_{rest} using the TH than using the library, while galaxies with bluer \$\mathbb{V}\$ Š \$V\$]_rest are shifted towards redder [/ S J]_{rest} colours – implying a shallower mid-IR pro le in solve this ambiguity, deeper data longward of the are necessary; this anticipates the need fdWSTobservations, which will be the target of Section 6.

Figure 7. In the top panel we show the shifts on tbb/J diagram of the objects in the reference sample, when tted with different libraries of models. Blue dots: exponentially declining (library; red squares: TH library. The colour. The bottom panels show two examples explaining the described trend: the tted SEDs substantially coincide in the optical - NIR, but differ in the IRAC region. See the text for more details. [A colour version of this gure is available in the online version.]

observed colour-colour planes, which are the equivalent observed diagram (Daddi et al2004) for selection of quiescent galaxies at z 3 andz 4. In each diagram, the upper right region (delimited by the diagonal solid line and the horizontal dashed line) is expected to be populated by passive sources. The grey dots are individual ob- $\stackrel{\circ}{ ext{9}}$ jects from the whole G13 catalogue, while red dots are galaxies having z_{CANDELS} in the interval of interest for the corresponding diagram. Larger lled dots are the reference sample sources, again a colour-coded depending on their photosee the caption of the colour-coded depending on their photosee the caption of the gure). While some of the selected objects lie in the passive region served colours. Therefore, a straightforward colour selection would exclude them from the sample (see Grazian e2007, for similar discussions on thezKselection).

Another interesting comparison can be made with the results from previous published studies. Rodighiero et 22007) used the Giavalisco et al. 2004 multiwavelength imaging data to extract all cases, as it can be seen in the two SEDs examples. To de nitively photometric data, performed a magnitude selection requiring no detection in HST bands K > 23.5, and IRAC 3.6 m < 23.26, and identi ed 20 objects as massive galaxies with high probability of being high-redshift, passive sources (with 14 of them also having

principle includes both star-forming and passive galaxies. Five objects in their selection also belong to our reference sample (IDs 2782, 7526, 12178, 17749, 18180). Of the other 11 objects in the N14 selection, 2 (IDs 9177 and 16671) have RNDELS < 3, one (ID 6189) is a low-redshift (CANDELS = 0.6) dust-obscured star-forming galaxy in the CANDELS catalogues while it is tted as a passive z = 4.0 object by N14, and eight (IDs 4356, 4624, 9286, 10479, 12360, 13327, 18694 and 19195) have star-forming best ts in our analysis: ve of them are also identi ed as AGNs in the catalogue by Cappelluti et al. 2016 (with three also included in the Xue et al.2011catalogue).

It is interesting to note that none of the previous cited works includes our best candidates, IDs 10578 and 22085, in their selections. S14 only include sources 23 \$\, 3.4, while ID10578 has $z_{CANDELS} = 3.06$ and ID22085 haz $c_{CANDELS} = 3.36$. On the other hand, both galaxies fail N14 colour selection criter MS J versus [H Š Ks]). In the case of ID22085J105 band photometry is not available in the CANDELS GOODS-South data set (this actually shows one more point of strength of the SED tting approach, in that the lacking of one band data does not compromise the whole study of one potentially interesting object); in ID10578, the object

breaks, blue band detections and rising FIR ux), and by the crosscorrelation with the 24 m catalogue by Magnelli et al2013, with 12 out of 18 objects having an association with au24 prior within 0.6 arcsec. Clearly the classi cation by Rodighiero et 2007) was heavily affected by the lower quality of the imaging data available at that time.

two of the most recent similar works, S14 and N14. S14 usl a criterion to single out six quiescent candidates in the GOODS-South (age> eld, which we cross-correlate with the G13 catalogue. Among these, three (CANDELS IDs 4503, 17749, 18180) belong to our rather high sSFR in the S14 t too (27x510S11, 18.6x 10S11 and 4.47x 10^{Š11} yr^{Š1}, respectively); they are also agged as probable AGNs in the Cappelluti et al. 2016 catalogue, and the rst two are identi ed as AGNs by Xue et al2011) as well; they all have con rmed spectroscopic redshift consistent with the NDFLS we use (Szokoly et al2004).

N14 identify 16 evolved (post-starburst) galaxies using & K colour selection to probe the 4000 Å break - a selection that in tion.

study of one potentially interesting object); in ID10578, the object falls immediately outside the selection area of their colour–colour diagram.

Figure 8. Diagnostic colour–colour diagrams. In both panels, grey dots are the whole G13 catalogue, and red dots are the sources havingers in the interval of interest for the corresponding diagnostic diagram/225
6 LOOKING FORWARD: THE JWST

PERSPECTIVE
As our study shows, there are still many sources of uncertainty that the selection uncertain: depending on the tightness of the selection criteria, one may end up with very different samples (e.g. in the lection criteria, one may end up with very different samples (e.g. in the lection criteria, one may end up with very different samples (e.g. in the lection criteria, one may end up with very different samples (e.g. in the lection criteria, one may end up with very different samples (e.g. in the lection criteria, one may end up with very different samples (e.g. in the lection criteria, one may end up with very different samples (e.g. in the lection criteria, one may end up with very different samples (e.g. in the lection criteria, one may end up with very different samples (e.g. in the lection criteria, one may end up with very different samples (e.g. in the lection criteria, one may end up with very different samples (e.g. in the lection criteria, one may end up with very different samples (e.g. in the lection criteria, one may end up with very different samples (e.g. in the lection criteria, one may end up with very different samples (e.g. in the lection criteria, one may end up with very different samples (e.g. in our case we can go from 30 to 2 objects). In particular, the spectral suge od accuracy the photometric redshift but especially to distinguish between the star-forming and passive objects, as, inferring the spectral slope both below and above the 4000 Å break demands a good coverage of the whole wavelength range from the redderSpitzebands, ideally up to §m.

The James Web

allowing for a detailed photometric reconstruction of the mentioned important spectral features and, hopefully, for a much easier disentanglement between degenerate solutions from SED-tting.

It is interesting to try a rough evaluation of the potential of the JWSTcapabilites in this context. To this aim, we have created a sample of synthetic spectra using our TH library. The full sample consists of 1686 simulated objects, of which 828 correspond We then check the correspondence between our selection and star-forming models (having age t_{burst}), 230 have quenched the SF activity since less than 100 Myr, and 628 are red and dead thurst + 100 Myr). Each of these spectra has been placed at redshifts from 3 to 7 (with the additional constraint that the age of the galaxy is not larger than the age of the Universe at that redshift) reference sample as well, while the other three (IDs 5479, 6294 at steps of 0.1 in redshift. We then created observational catalogues and 19883) have a star-forming best t. Indeed, they are assigned corresponding to such models, reproducing both the Iter sequence and depths of the CANDELS catalogue used in this work, as well as an idealized catalogue reproducing a possible survey executed with JWST To this purpose we have replaced all the CANDELS Iters redward of Y (included) with a combination of 12WST

⁴ See the webpage

for full informa-

Figure 9. Comparison of the VJ diagrams from mock observed catalogues, where the rest-frame magnitudes are obtained via SED- tting using CANDELS (left panels) and WST(right panels) Iter sets. The mock catalogues have been created starting from the TH library of spectra, simulating 1686 objects including passive and star-forming galaxies, computing the observed uses in all the relevant bands proceed to three reference are including to the content of the (left panels) and/JWST(right panels) Iter sets. The mock catalogues have been created starting from the TH library of spectra, simulating 1686 objects including passive and star-forming galaxies, computing the observed uxes in all the relevant bands rescaled to three reference magnitudes (leach rogure corresponds to one of them – from top to bottom, smm = 23, 24 and 25), and including observational noise. In each panel, models having ongoing SF including passive and star-forming galaxies, computing the observed uxes in all the relevant bands rescaled to three reference magnitudies (leach ro activity in the input library are plotted as blue stars, recently quenched objects as green squares, and passively evolving galaxies as reastdets limbs d de ne a 'green valley' used to quantify the contamination between the different samples. It is clear that The ass-bands set removes almost completely the contamination in the tted colours between the three different populations, which is severe in the CANDELS case. See the text for more debails. [A c version of this gure is available in the online version.]

bands F090W, F115W, F150W, F200W, F277W, F356W, F444W, F560W, F770W, F1000W, F1130W and F1280W), as described in the MIRI and NIRCam documentation webpages. The resulting catalogue mimicks a survey executed (redward of F090) with ST on the GOODS-S eld, building upon the existent ACS data. In tudes to three reference values, 5 um = 23, 24 and 25, covering the magnitude range of our candidates. Noise has been added to IWSTlike catalogues separately. They are shown in Bigfor these catalogues accordingly to the observed S/N versus magnitudall objects having 3 z_{ohot} < 7. In each panel, models having relation in the CANDELS Iters (see Castellano et 2012: in the in Finkelstein et al. 2015). For the three reddestWST lters that of the otherJWST Iters.

photomeric redshifts and SED properties from the SED- tting, and magnitudes 14,511 m = 23, 24 and 25, the CANDELS simulation, re-(b) because we ignore, on the one hand, the additional gain to spectively, yields 3.6, 7.2 and 10.0 per cent star-forming galaxies resolution of JWST compared to Spitzer, and on the other hand any possible complication due to the blending of sources and other cases are 3.0, 16.7 and 31.4 per cent.

systematics. Regardless of these limitations, these tests can give us a preview of the improvements that VST will make possible.

preview of the improvements that VST will make possible.

We have repeated on these simulated catalogues the same analysis that ysis that we did on real data. We rst tted catalogues with our SED-tting code, and then computed the rest-frame properties particular, we created three catalogues by normalizing the magni- at the photometric redshift. For simplicity, we show here the results obtained in the UVJ plane, for the CANDELS-like and the ongoing SF activity in the input library are plotted as blue stars, JWSTsimulated bands, we have assumed the depth expected in the ecently quenched objects as green squares, and passively evolvcase of an extragalactic survey for high redshift galaxies describeding galaxies as red dots. The results on the CANDELS simulated data show that there is a strong contamination in the t, as were included there, we have computed the expected signal-to-noisemany passive and star-forming galaxies end up in the same reratio assuming a total exposure time per liter comparable to each gions of the UVJ diagram. For example, one can de ne a 'green valley' as the region of the diagram for which S J > 0.5 and These simulations are clearly simpli ed, since (a) they use the 0.88x [VŠJ] + 0.44< UŠV < 0.88x [VŠJ] + 0.69 (see the

same library to compute the 'true' galaxy colours and to derive their dashed lines in Figh: considering the three data sets with reference the overall photometry that will be possible using the improved erroneously falling within or above the green valley; conversely, the passive models falling within or below the green valley in the three

MNRAS 473,2098-2123 (2018)

ies are fainter. This simulation con rms that the identi cation of passive galaxies in the CANDELS data set is potentially prone to (2016) new catalogue based on detected priors. Two objects in

Conversely, the situation is much more de ned using JIMEST Iters: the three populations are robustly tted and separated, with (Xue et al 2011; Cappelluti et al 2016); we therefore speculate that put true colours, which the tted ones closely resemble). This is with an FIR source. an exciting demonstration of the future capabilities with the new instrument.

passive region of the diagram, as discussed in the previous sectionssSFR< 10^{\$11} yr^{\$1}). Five objects are in common between this sethis shows again how the VJ colour selection can be prone to the risk of missing objects that have guenched their SF activity in recent 18180). times, even using a much more accurate photometric data set.

7 SUMMARY AND CONCLUSIONS

mary of the work is the following.

- (i) We search for high-redshift, red and dead (i.e. passively evolving) galaxies in the GOODS-South eld, using an updated version of the Guo et al. 2013 photometric catalogue that includes CAN-DELS HST uxes, HUGS Ks data, and new IRAC images and improved photometric measurements (Section 2). We pre-select detected objects havinks, IRAC 3.6 and 4.5 um 1 detection, and ZCANDELS > 3. We also add a new sample of 1K8/RACdetected sources from Boutsia et al. (in preparation) and Wang viding them by the age of the Universe at the time the SF activity et al. (2016).
- (ii) We then analyse this selection using dedicated-hat libraries for SED-tting. We assume that a single star formation event took place and abruptly stopped in the past, followed by passive evolution ever since, and we t the observed uxes with models having different values for the duration of the burst, the UV extinction and the metallicity. The selection critemust have at least one passive model solution (i.e. SFR) and age larger than the burst duration) with 2) > 30 per cent, and do not have any star-forming solution with a probability $p(^2) > 5 per cent.$
- (iii) We rst use a library without nebular lines emission and only consider the CANDELS redshifts. This way we select 30 candidates, all of which areH-detected (see Fig8.1 and C1).
- (iv) Including nebular lines in the top-hat library used for the SED-tting procedure, only 10 of these candidates surweaken the tted continuum redward of the 4000 Å break, vielding a star-forming best-t: in other cases, the probabilissolutions.
- (v) If we repeat the analysis letting the redshift free to vary around the best-tting value, only two galaxies (IDs 10758 and 22085) retain their passive status as the only robust solution. All the other objects show alternative star-forming solutions (at different redshifts) with a probability $p(^2) > 5$ per cent.
- (vi) Since it is not possible to completely rule out strongly (see Fig. D1), as a basic sanity check we perform a crosscorrelation of the reference sample with the 124 catalogue by

This contamination increases (as expected) when input galax-Magnelli et al. 2013, on HerschelPEP-GOODS (Lutz et a2011) and HerMES (Smith et a2012) blind catalogues, and on Wang et al. misidenti cation due to the still inadequate depth of the photometry. our selection are associated with strong FIR emitters. Interestingly, they are also identi ed as optical counterparts Xofay emitters almost no contamination even down to the faintest magnitudes (the they might be recently quenched galaxies, hosting a dust-obscured observed 'arched' distributions on the diagram derive from the in- AGN. No other object in the reference sample has a clear association

(vii) By means of a direct selection on the full G13 catalogue using a standard exponential models t with BC03, we then identify. It is interesting to note that some red objects again fall outside the for comparison, 10 sources 25 3 passive candidates (we require lection and the reference sample (IDs 2782, 7526, 8785, 17749, \$\sigma\$

A clear outcome of our analysis is that the selection of passive galaxies, at least in the considered range of redshifts, is still prone to signi cant uncertainties, due to the limitations in the assumptions used in the SED tting models and the relatively modes of the In this paper we have presented the methods and results of a study bjects. Nevertheless, considering the weakest among our selections aimed at searching passive galaxies in the early Universe. The sum-criteria, we can at least derive an upper limit for the number density of these objects, nding 0.173 arcmin (or 2.0 x 10 5 Mpc 3 for 3 < z < 5).

The limitations in the SED modelling hampers our chances to derive robust physical information on the selected sample. Ages are poorly constrained, and thus so are the SF rates necessary to assemble such objects. We can try some educated guess on the mine imum sSFR of the selected sources (assuming isolated evolution,∃ i.e. no mergers) by taking their estimated stellar masses, and dividing them by the age of the Universe at the time the SF activity ceased (minus 300 Myr, to crudely exclude the dark ages), in the least ting models (we consider the t without nebular lines, for simplicity). This yields a typical lower threshold for the sSFR of 17 to 10 10 yr 10 y $7 \times 10^{\$10} \text{ yr}^{\$1}$, which is fairly consistent with the observed values of main-sequence star-forming galaxies, in the same redshift and mass regimes (e.g. Salmon et2a)15 Schreiber et al2017). This is the sSFR estimated the endof the activity, i.e. when the rion is based on two stringent requirements: the selected objects mass has been completely assembled; we note that, since in our scheme the rate of star formation of the models is constant before the quenching, if we had observed the galaxies during the star formation phase they would have been classi ed as starbursts, because having lower stellar mass they would beovethe Main Sequence 2 M Š M relation.

By means of a dedicated simulation, we have shown JNOWST will yield a major improvement in this perspective, allowing for a much more effective detachment of higheassive objects from dust-obscured low-ones, thanks to an effective coverage of crucial vive the probabilistic selection process: in many cases, the lines regions of the observed spectra - namely, the 4000 Å break and the 20 µm rest-frame regions.

A thorough testing against theoretical expectations for the numtic approach causes the exclusion of galaxies with alternative ber density and properties of these kind of objects, at the considered redshifts, is compelling and recommended.

ACKNOWLEDGEMENTS

The research leading to these results has received funding from the European Union Seventh Framework Programme (FP7/2007-2013) obscured star-forming solutions for any of the selected sources under grant agreement no. 312725. We thank the anonymous referee for the useful comments and suggestions, which greatly helped to improve the paper.

REFERENCES Anders P., Fritze-von Alvensleben U., de Grijs R., 2003, Ap&SS, 284, 937 Ashby M. L. N. et al., 2015, ApJS, 218, 33 Brammer G. B., van Dokkum P. G., Coppi P., 2008, ApJ, 686, 1503 Brammer G. B. et al., 2009, ApJ, 706, L173 Bruzual G., Charlot S., 2003, MNRAS, 344, 1000 Calzetti D., Armus L., Bohlin R. C., Kinney A. L., Koornneef J., Storchi-Bergmann T., 2000, ApJ, 533, 682 Cappelluti N. et al., 2016, ApJ, 823, 95 Cassata P. et al., 2015, A&A, 573, A24 Castellano M. et al., 2012, A&A, 540, A39 Castellano M. et al., 2014, A&A, 566, A19 Castellano M. et al., 2016, A&A, 590, A31 Ciesla L. et al., 2016, A&A, 585, 43A Cimatti A. et al., 2004, Nature, 430, 184 Daddi E., Cimatti A., Pozzetti L., Hoekstra H.öRgering H. J. A., Renzini A., Zamorani G., Mannucci F., 2000a, A&A, 361, 535 Daddi E., Cimatti A., Renzini A., 2000b, A&A, 362, L45 Daddi E., Cimatti A., Renzini A., Fontana A., Mignoli M., Pozzetti L., Tozzi P., Zamorani G., 2004, ApJ, 617, 746 Daddi E. et al., 2005, ApJ, 626, 680 Dahlen T. et al., 2013, ApJ, 775, 93 Dickinson M., Papovich C., Ferguson H. C., BudavT., 2003, ApJ, 587, Feldmann R., Quataert E., Hopkins P. F., Faucher-@ig@C.-A., Kere D., 2017, MNRAS, 407, 1050 Finkelstein S. L., Dunlop J., Le Fevre O., Wilkins S., 2015, preprint Fontana A., D'Odorico S., Poli F., Giallongo E., Arnouts S., Cristiani S., Moorwood A., Saracco P., 2000, AJ, 120, 2206 Fontana A. et al., 2004, A&A, 424, 23 Fontana A. et al., 2006, A&A, 459, 745 Fontana A. et al., 2009, A&A, 501, 15 Fontana A. et al., 2014, A&A, 570, A11 Giallongo E. et al., 2015, A&A, 578, A83

Giavalisco M. et al., 2004, ApJ, 600, L93 Grazian A. et al., 2006, A&A, 449, 951 Grazian A. et al., 2007, A&A, 465, 393 Grazian A. et al., 2015, A&A, 575, A96 Grogin N. A. et al., 2011, ApJS, 197, 35 Guo Y. et al., 2013, ApJS, 207, 24 Ilbert O. et al., 2013, A&A, 556, A55 Koekemoer A. M. et al., 2011, ApJS, 197, 36 Labbé I. et al., 2005, ApJ, 624, L81 Labbé I. et al., 2015, ApJS, 221, 23 Laidler V. G. et al., 2007, PASP, 119, 1325 Lutz D. et al., 2011, A&A, 532, A90 Magnelli B. et al., 2013, A&A, 553, A132

Merlin E., Chiosi C., Piovan L., Grassi T., Buonomo U., Barbera F. L., 2012, MNRAS, 427, 1530 Merlin E. et al., 2015, A&A, 582, A15 Merlin E. et al., 2016, preprint () Mobasher B. et al., 2005, ApJ, 635, 832 Muzzin A. et al., 2013, ApJ, 777, 18 Nayyeri H. et al., 2014, ApJ, 794, 68 Paci ci C. et al., 2015, MNRAS, 447, 786 Papovich C., Dickinson M., Ferguson H. C., 2001, ApJ, 559, 620 Patel S. G., Holden B. P., Kelson D. D., Franx M., van der Wel A., Illingworth G. D., 2012, ApJ, 748, L27 Pozzetti L., Mannucci F., 2000, MNRAS, 317, L17 Prevot M. L., Lequeux J., Prevot L., Maurice E., Rocca-Volmerange B., 1984, A&A, 132, 389 Rodighiero G., Cimatti A., Franceschini A., Brusa M., Fritz J., Bolzonella M., 2007, A&A, 470, 21 Rosati P., Stanford S. A., Eisenhardt P. R., Elston R., Spinrad H., Stern D., Dey A., 1999, AJ, 118, 76 Salmon B. et al., 2015, ApJ, 799, 183 Salpeter E. E., 1959, ApJ, 129, 608 Santini P. et al., 2012, A&A, 538, A33 Santini P. et al., 2015, ApJ, 801, 97 Schaerer D., de Barros S., 2009, A&A, 502, 423 Schaerer D., Vacca W. D., 1998, ApJ, 497, 618 Schaye J. et al., 2015, MNRAS, 446, 521 Schreiber C., Pannella M., Leiton R., Elbaz D., Wang T., Okumura K., Leabb I., 2017, A&A, 599, A134 Silk J., Mamon G. A., 2012, Res. Astron. Astrophys., 12, 917 Smith A. J. et al., 2012, MNRAS, 419, 377 Sommariva V. et al., 2014, A&A, 571, A99 Stefanon M., Marchesini D., Rudnick G. H., Brammer G. B., Whitaker K. E., 2013, ApJ, 768, 92 Straatman C. M. S. et al., 2014, ApJ, 783, L14 Szokoly G. P. et al., 2004, ApJS, 155, 271 van Dokkum P. G. et al., 2004, ApJ, 611, 703 Vanzella E. et al., 2008, A&A, 478, 83 Vogelsberger M. et al., 2014, MNRAS, 444, 1518 Wang T. et al., 2016, ApJ, 816, 84 Whitaker K. E. et al., 2011, ApJ, 735, 86 Whitaker K. E. et al., 2013, ApJ, 770, L39 Wiklind T., Dickinson M., Ferguson H. C., Giavalisco M., Mobasher B., Grogin N. A., Panagia N., 2008, ApJ, 676, 781 Williams R. J., Quadri R. F., Franx M., van Dokkum P., Lébb 2009, ApJ, 691, 1879 Wuyts S. et al., 2007, ApJ, 655, 51 Xue Y. Q. et al., 2011, ApJS, 195, 10

Maiolino R. et al., 2008, A&A, 488, 463 Marchesini D. et al., 2010, ApJ, 725, 1277

APPENDIX A: PHYSICAL PROPERTIES OF THE SELECTED SAMPLE OF RED AND DEAD CANDIDATES

to the reference sample, as obtained from their best t with the TH library line t. without emission lines. IBANDELS is the identi cation number in the G13 cataloguez_{CANDELS} is the of cial CANDELS redshift. ²_{reduced} is the normalized (reduced) ² of the best t. The SFR is always zero, by de nition. The table lists rst the two most robust candidates, which have passed all the selection criteria including the freet; second, the other 8 objects, identi ed as passive in the emission line t as well (see Tabia); nally, the remaining 20 objects in the reference sample.

ID _{CANDELS}	ZCANDELS	2 reduced	Age (Gyr)	Stellar mass (f0M)
10578	3.06	1.97	. 6 3 ⁺ 0.37 5 0.31	239.70 ^{+ 108.80} 554.40	
22085	3.36	1.26	. 6 1 ⁺ 0.97 50.30	44.25 ⁺ 17.08 5 12.31	
2717	3.04	1.13	.158 ^{+ 0.00} 5 0.97	16270 56.80 569.01	
2782	3.47	0.94	. 0 1 ^{+0.88} 50.40	69.95 ⁺ 16.27 \$ 26.15	
3912	4.08	1.32	. 25 ^{+ 0.05} 5 0.94	36.27 ^{+ 25.08}	
8785	3.98	0.72	.91 ⁺ 0.39 50.59	38.96 ^{+ 17.36} 5 15.65	
9209	4.55	1.61	. @11 † 0.74 Š 0.21	91.51 ^{+ 27.69}	
17749	3.73	0.63	. 9 05 0.40	108.80 ^{± 30.20} 5 _{51.19}	
18180	3.61	1.36	. 91 ^{+ 0.39} Š 0.50	90.11 ^{+22.29}	
23626	4.64	1.05	. @1 †0.69	75.91 ^{+ 28.89} \$25.90	
2608	3.58	1.36	. 663 ^{+ 0.42} Š 0.43	4.51 ⁺ 1.23 5 1.83	
3897	3.14	1.12	. 36 + 0.69 Š 0.16	11.86 ^{+ 10.14}	
3973	3.67	1.84	. 9 1 ⁺ 0.39 50.30	186.10 ± 16.40 ± 85.20	
4503	3.52	3.74	. 11 0 ^{+ 0.20} Š 0.80	14270 ^{± 38.20} 5 _{59.61}	
4587	3.58	2.55	. @11 ^{+ 0.85} 5 0.21	5.48 ^{+ 4.34} 5.1.72	
5592	4.45	1.05	. 36 + 0.79 Š 0.16	30.16 ^{+ 17.90}	
6407	4.74	1.31	. 36 ^{+ 0.69} 5 0.16	15.98 ^{± 11.26}	
7526	3.42	0.60	. 9 0 <u>+</u> 0.68 5 0.58	36.24 ^{± 17.89} 3 _{517.45}	
7688	3.35	0.69	. 661 ^{+ 0.97} Š0.31	22.76 ^{+ 12.09}	
8242	3.18	1.17	. 100 ^{+ 0.58} 5 0.69	6.55 ^{+ 1.97}	
9091	3.30	2.22	. 36 + 0.90 5 0.16	2.81 ^{+2.69} _{50.81}	
10759	3.07	1.38	. 6 3 ⁺ 0.95 5 0.62	$0.91^{+1.17}_{50.64}$	
12178	3.28	1.02	. 1 0 ⁺ 0.20 50.79	41.20 [±] 16.64 5 10.46	
15457	3.41	1.98	. G 6 ^{+ 0.69} Š 0.16	$4.39^{+2.90}_{50.63}$	
16506	3.34	3.68	. G 6 ^{+ 0.69} Š 0.16	5.06 ^{+ 3.62} 5.06 ^{+ 3.62}	
19301	3.60	2.85	. 1 0 ⁺ 0.20 5 0.90	11.58 ^{+ 7.36} 5.39	
19446	3.25	2.89	. 10 0 ± 0.58 0.80	20.07 [±] 3.37 \$10.73	
19505	3.33	1.20	. 6 3 ⁺ 0.57 5 0.43	46.63 ⁺ 6.19 5 15.00	
22610	3.22	0.74	. 6 3 ⁺ 0.63 5 0.43	9.49 ^{± 4.40} \$3.09	
26802	3.45	1.75	. 6 3 [±] 0.95	4.67 ^t 2.45 31.92	

Table A2. Physical properties of the 10 red and dead candidates passing the probabilistic selection including nebular lines emission in the to ADDELS is the identi cation number in the G13 cataloguze; ANDELS is the of cial CANDELS redshift. $^2_{reduced}$ is the normalized (reduced) 2 of the best t. The SFR is always zero, by de nition. The table lists rst the two most robust candidates, which have passed all the selection criteria including the Table A1. Physical properties of the red and dead candidates belonging freez t; then, the other eight objects identi ed as passive in the emission

ID _{CANDELS}	ZCANDELS	2 reduced	Age (Gyr)	Stellar mass (190M
10578	3.06	1.97	. 6 3 ⁺ 0.37 Š 0.47	239.60 ^{+ 108.70}
22085	3.36	1.26	. 6 1 ⁺ 0.97 5 0.59	44.23 ^{± 17.04} \$33.61
2717	3.04	1.13	.158 ^{+ 0.00} 5 0.97	16250 \$ 56.70 \$ 62.89
2782	3.47	0.94	Ø150.40	69.90 ^{+ 16.26} 526.12
3912	4.08	1.32	. 125 ^{+ 0.05} 5 0.94	36.26 ^{+ 25.07} 5 15.78
8785	3.98	0.72	. 91 ^{+ 0.39} Š 0.59	38.95 ^{+ 17.35} 5 15.65
9209	4.55	1.61	Ø41 ^{+ 0.74} Š 0.40	91.49 ^{± 27.61}
17749	3.73	0.63	. 9 05 0.40	108.80 ^{+30.10} 551.29
18180	3.61	1.36	. 9 1 ⁺ 0.39 S 0.50	90.04 ^{+, 22.26} 38.04
23626	4.64	1.05	. 41 [±] 0.69 5 0.11	75.88 ^{+ 28.92} 525.89

APPENDIX B: SNAPSHOTS OF THE TH CANDIDATES

Figure B1. Snapshots of the 30 passive candidates selected in the reference sample, obtained with the TH library. LefAccriBf435 + V606 + I814 stack, WFC3 J125, WFC3 H160, Hawk-IKs, IRAC 3.6 + 4.5 μm stack, IRAC 5.8 + 8.0 μm stack. [A colour version of this gure is available in the online version.]

APPENDIX C: SEDS OF THE TH REFERENCE SAMPLE CANDIDATES

Figure C1. SED- tting for the objects in the reference sample. Shown is the best t using the TH librariesz with (red line) and without (black line) the inclusion of nebular emission; in many cases the two ts almost coincide, so the two lines are superposed. The physical parameters of t best- tting models are reported on the bottom of each plot, with colours (blue or black) corresponding to the considered t. [A colour versiog wifetings available in the online version.]

Figure C1 - continued

APPENDIX D: PROBABILITY AND EXTINCTION OF ALL THE MODEL SOLUTIONS OF THE TH CANDIDATES

Figure D1. Probability and dust extinction as a function of [to burst] for all the possible solutions in the SED- tting process, for all the candidates in the TH selection. For each candidate, indicated by its ID, two panels are shown. In the upper one, dots represent the probabilities had model solution; the colours of the dots refer to the belonging of the source to the selection with (blue) or without (red) the inclusion of nebular lines; the dots (delst) heren shaded as a function of their density. The lower one shows the corresponding value (stress). All the solutions have age to burst as required to be classified as passive in this approach. Galaxies excluded from the selection, on the other hand, have been tited by at least one model with saighest still star-forming, with a probability > 5 per cent (not shown). [A colour version of this gure is available in the online version.]

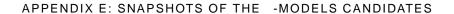


Figure E1. Snapshots of the ve passive candidates selected with threedels library which are not present in the reference sample. Left to AGS B435+ V606+ I814 stack, WFC3 J125, WFC3 H160, Hawk-IKs, IRAC 3.6+ 4.5 μ m stack, IRAC 5.8+ 8.0 μ m stack. [A colour version of this gure is available in the online version.]

This paper has been typeset from XTATEX le prepared by the author.